SAE International Journal of Aerospace, Volume 19, Issue 2, May 2025, Article number 01-18-02-0008
DOI:10.4271/01-18-02-0008

Impact of high aspect ratio wing aircraft concepts on conventional tricycle landing gear integration

Raphaël Martin[1], Jack Stockford[2], and Howard Smith[3]
Cranfield University, Bedford, MK43 0AL, United Kingdom

April 17, 2025

Abstract

To comply with the Paris agreement targets set in 2015, significant reductions in aircraft emissions are required. This demands a fundamental shift in aircraft design. Therefore, it is essential to study how future aircraft designs will affect the integration and design of landing systems. This research project examines the landing gear issues that arise from adopting specific future aircraft configurations. The study focuses on two primary configurations: the High Aspect Ratio Wing and the Ultra-High Aspect Ratio Wing, with selected aircraft concepts from Cranfield University as baselines. It investigates the design and integration of conventional landing systems into these new aircraft concepts, highlighting the limitations posed by the modified airframes. The selected concepts include either telescopic or trailing arm arrangements, with attachment points on the wings or fuselage. A methodology for preliminary sizing of landing systems is presented, emphasizing automation and determining key performance indicators to assess the suitability of each solution for different aircraft architectures. The challenges of these novel airframes highlight opportunities to move away from conventional solutions and explore unconventional methods of interfacing between the aircraft and the ground.

Keywords

Landing gear design, high aspect ratio wing, fuselage, trailing arm, design framework, weight estimation, fuel penalty, structural integration.

[1] Corresponding author. E-mail: raphael.martin@mines-albi.org
[2] Lecturer in aircraft design, School of Aerospace Transport and Manufacturing
[3] Professor of aircraft design, School of Aerospace Transport and Manufacturing

Published by [Publisher]. This is the Author Accepted Manuscript issued with: Creative Commons Attribution License (CC:BY 4.0).
The final published version (version of record) is available online at DOI:10.4271/01-18-02-0008. Please refer to any applicable publisher terms of use.

Nomenclature

ACN	Aircraft Classification Number
$AGIS$	Aircraft/Ground Interface Solution
$ALCAS$	Advanced Low-Cost Aircraft Structures
AVD	Aerospace Vehicle Design
BWB	Blended Wing Body
CAD	Computer-Aided Design
CFD	Computational Fluid Dynamics
CG	Center of Gravity
DL	Design Landing
FEA	Finite Elements Analysis
GDP	Group Design Project
HAR	High Aspect Ratio
$ICAO$	International Civil Aviation Organization
$LGPDF$	Landing Gear Preliminary Design Framework
MLG	Main Landing Gear
MLM	Maximum Landing Mass
$MTOM$	Maximum Take-off Mass
NLG	Nose Landing Gear
PCN	Pavement Classification Number
RF	Reserve Factor
RTO	Rejected Take-O
SLS	Safran Landing Systems
$UHAR$	Ultra-High Aspect Ratio
VAT	Vertical Axle Travel

1 Introduction

Project Background

In view of mitigating the catastrophic consequences of climate change [1,2], the Paris Agreement from 2015 set a target of a 1.5°C maximum increase in global average temperature above pre-industrial levels [3]. To achieve this ambitious goal, the key challenge will be to drop the CO_2 emissions to net-zero by mid-century as stated by the Intergovernmental Panel on Climate Change [4].

Aviation accounts for 2% of all human-induced CO_2 emissions, and 12% of the emissions from all transport sources [5]. In order to reach global net-zero, the specific targets set for the aerospace sector are to achieve carbon-neutral growth from 2021 and reduce its net emissions to half of 2005 levels by 2050 [6]. This will have to be combined with the predicted constant 4% annual growth of the aviation sector, leading to a doubling in passenger numbers between 2016 and 2036 [7].

Several studies established that the incremental improvements in fuel efficiency from individual technological bricks (engines, materials, operations management ...) will not be sufficient to achieve these targets while keeping the current growth rate. A fundamental shift in aircraft design will be required, and novel aircraft concepts will emerge over the next decades to enable this drastic drop in net emissions [7,8]. When considering the 2035 timeframe, the most likely configurations will feature high-aspect ratio wings fitted on a traditional fuselage (see Figure 1). Revolutionary concepts such as the Blended Wing Body present many more technical and economic risks and are therefore likely to be developed further in the future [9].

The future generation of aircraft will present different geometries and structural layouts, driving potential changes to the integration of sub-systems such as the landing gear. This research project, funded by Safran Landing Systems, explored the potential challenges arising from future airframes and suggested solutions for the integration of landing systems.

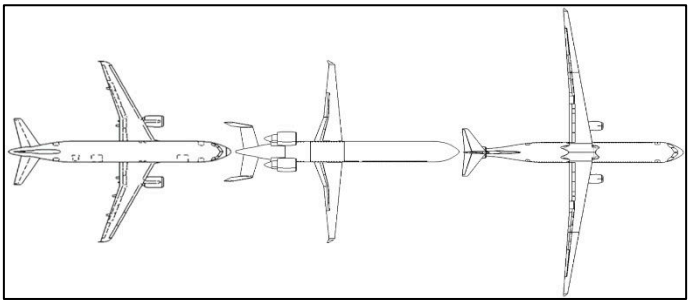


Figure 1. Potential evolution towards high aspect ratio wings from Airbus A320 baseline

Existing research

New aircraft architectures can potentially affect the integration of all subsystems, including the landing gear, which will generate new challenges and could require the implementation of unconventional solutions. In such cases, statistical design data become obsolete, and novel design methods need to be investigated. Even though this issue was mentioned in the late 1980's when testing analytic weight estimations methods on unconventional landing gear layouts [10], not much work has been done to further develop this area until recent years. When considering future aircraft concepts, such as high aspect ratio wings or blended wing body architectures, most of the work focused on airframe design and propulsion

considerations, with little investigation of the implications for the landing system. This observation led to the development of an analysis framework for BWB aircraft concepts to compare several landing gear configurations and study the impact of the ground loads distribution [11]. Another project looked at a fuselage-mounted landing gear for the Prandtl Plane transport aircraft, featuring two telescopic 4-wheels bogies retracting forward into fuselage pods [12]. The main published work considering landing systems for HAR concepts is the comparison of wing-mounted versus fuselage-mounted gears on an aircraft featuring low-mounted wings with engines on top of them [13,14], a performance analysis of various aircraft architectures (including landing gear integration) [15], and the aerodynamic design of a narrow-body airliner with a fuselage-mounted landing gear which does not investigate other integration options [16].

Aim and objectives

The research described in this paper builds upon the work of Kling et al. [13] by developing a refined design framework and applying it to compare different landing system solutions integrated into two distinct aircraft configurations. This aim is decomposed into the following set of discrete objectives:

1. Selection of relevant aircraft architectures
2. Selection of landing system configurations
3. Analysis of the selected configurations through the design framework
4. Comparison of key performance indicators resulting from the design framework

Based on the results obtained, the challenges raised by future aircraft architectures will be discussed and corresponding technological solutions will be proposed.

2 Methodology

2.1 Aircraft concepts selection

As mentioned in the introduction, the investigation in future aircraft concepts led to configurations featuring high and ultra-high aspect ratio wings. Two specific aircraft concepts were selected to further define the project scope by reducing the number of parameters to consider and focus on the landing gear integration. Both aircraft were designed as part of the Group Design Project of the Aerospace Vehicle Design MSc at Cranfield University, which is a six months long teamwork project recreating a virtual industrial environment [17]. It produced (among other outputs) a detailed structural layout of the fuselage and wings. The following paragraphs provide an overview of these two aircraft concepts, which are both medium-range airliners featuring a maximum take-off mass of around 87 metric tons.

Low-mounted high aspect ratio wing Cranfield Ae-16

The Ae-16 "Aurora" is a hybrid-electric airliner designed by the AVD 2016/2017 team. It is a revolutionary aircraft concept designed to lead the family of short-to-medium range narrow-body jet airliners into a new era of aviation. The concept exploits numerous emerging aerospace technologies in the global pursuit of meeting aviation environmental targets. Aside from the hybrid electric propulsion, this aircraft features a high-aspect ratio wing with natural laminar ow airfoil, elliptic-section fuselage, and state-of-the-art airframe systems.

High-mounted ultra-high aspect ratio wing Cranfield A-17
The A-17 "Zephyr" is an advanced technology low-drag airliner designed by the AVD 2017/2018 team. The aircraft is similar in passenger capacity and range to a Boeing 737 or an Airbus A320 and is targeting an entry into service in the 2030-2035 timeframe. It includes advanced technologies to reduce the impact on the environment and lead a new generation of greener aircraft. Key features of the A-17 include an ultra-high aspect ratio wing and a boundary layer ingestion aft propeller which provides a third of the thrust at cruise and numerous more-electric technologies. Designs have been optimized to reduce noise and emissions and to improve passenger comfort through the elliptical shape of the fuselage and the design of a spacious cabin.

2.2 Landing system solution selection

After identifying these two reference aircraft concepts, a design space exploration of the aircraft/ground interface solutions is conducted for each of them. The AGIS denomination is employed as a generalization of the "landing gear" or "undercarriage" terms to include the potentially very unconventional concepts considered. Some of these solutions are inspired by a survey of existing landing systems and adapted to the novel aircraft concepts, while others drift away from the conventional wheel-based systems. The set of identified solutions is then narrowed down by assessing their compliance with the functional requirements of an AGIS, and the remaining landing systems are graded and ranked using a decision-matrix method to select only the top-scoring ones for further detailed studies. The set of criteria used to rank the solutions and the associated weightings (provided by SLS based on their experience in the field) are:

- Cost and manufacturing (35%)
- Performance and design (25%)
- Operation (15%)
- Maintenance (15%)
- Environmental awareness (10%)

It can be noted that a dedicated “Safety” criterion is not explicitly listed in the decision matrix. However, it is included in the two top-ranking secondary attributes of the “Operation” category: “Fault tolerance” and “Operability”. Moreover, a general safety compliance would have been difficult to establish due to the low level of details at this conceptual stage. Specific safety aspects can be addressed with specific technological solutions once the design is more mature.

The final selection of concepts is presented below for each of the aircraft configurations.

2.2.1 Ae-16 solutions

Wing-mounted telescopic landing gear
The baseline landing system for this aircraft configuration is adapted from the Airbus A320 layout. The main landing gears are composed of twin wheels connected to the inner wing by a telescopic strut, as shown on the left-hand side of Figure 2. The main wheels retract inward into the fuselage belly fairing. The nose landing gear is composed of a steerable pair of twin wheels mounted on a telescopic strut and retracts forward into the fuselage.

Low-wing fuselage mounted trailing arm landing gear
This concept adapts the BAe-146 fuselage mounted gear arrangement to a low-wing aircraft. The main landing gear consists of two pairs of twin wheels in a trailing arm configuration, as shown on the right-hand side of Figure 2. The wheels retract inward into the fuselage belly fairing. The system features a shortening mechanism to minimize storage volume.

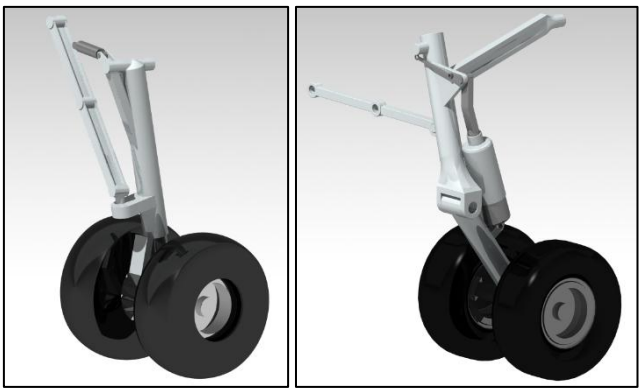


Figure 2. Ae-16 landing gear solutions (left: wing-mounted telescopic; right: fuselage-mounted trailing arm)

2.2.2 A-17 solutions

High-wing fuselage mounted trailing arm landing gear
The baseline landing system for this aircraft configuration is adapted from the BAe-146 layout. The main landing gear is composed of two pairs of fuselage-mounted twin-wheels in a trailing arm configuration, as shown on the left-hand side of Figure 3. Both units retract inward into the fuselage, using a shortening mechanism to fit inside the belly fairing. The nose landing gear is a single pair of twin-wheels mounted on a telescopic strut and retracts forward into the fuselage.

Rotating telescopic tandem landing gear
This concept is based on the TSR-2 landing gear. The main units are two pairs of tandem wheels attached to the fuselage by telescopic struts, as shown on the right-hand side of Figure 3. The gear can either retract forward or backward into the fuselage. The added rotating motion around the longitudinal axis to turn the wheels down allows storage without an additional fairing.



Figure 3. A-17 landing gear solutions (left: trailing arm; right: telescopic)

2.3 Design framework

To compare the performance of each landing system solution, a design framework is set-up following traditional preliminary design activities while attempting to automate as many design steps as possible. The integration aspects will require details about the aircraft structure, which is where the use of existing GDP aircraft concepts will bring a major added value. These aircraft have been fully designed by large teams of students, and the results feature a high level of detail including a fully sized airframe structure. The different steps of the design method are described in this section, and an overview of the framework is provided in Figure 4. This tool will be referred to as the Landing Gear Preliminary Design Framework in the following.

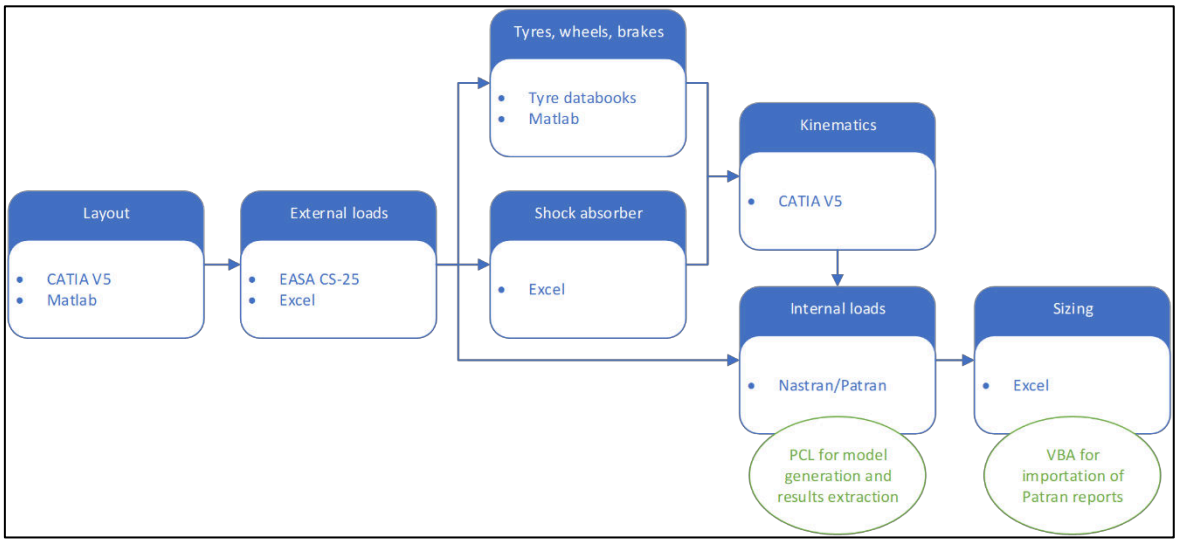


Figure 4. Summary of the design framework

2.3.1 Initial layout

The landing gear configuration (number of struts, mounting locations) is provided by the initial concept description. From there, and using aircraft level parameters, the precise position of the ground contact points is determined. This positioning process must respect a set of requirements to ensure safe and stable ground operations of the aircraft, described below for the case of a nose gear configuration.

Tip-back angle

This angle is measured between the line connecting the aft-most center of gravity position and the MLG ground contact point, and the vertical. As stated by N.S. Currey [18], this angle must be at least 15 to ensure that the aircraft will not tip-back onto its tail when in a nose-up pitching attitude.

Tail-down angle

This requirement combines the aircraft geometry and the take-off /landing performance characteristics. It is measured between the static ground line and the aft fuselage pro le and limited by the maximum pitching angle required for take-off /landing. The aim is to prevent contact between the aft fuselage or tail and the ground during take-off and landing. When the actual maximum pitching angle required is unknown, a value of 15° is advised as a conservative first estimate. For both aircraft concepts, the performance studies conducted during the GDP

mentioned in section 2.1 resulted in a pitching angle requirement of 10°, which will be used as critical value for tail-down angles.

Turnover angle
This is a ground stability criterion, ensuring that the aircraft can handle side-loads due to wind gusts and turns while on ground. This can become a critical design driver for the landing gear track in the case of high CG locations (high-wing aircraft for example). The method for calculating this angle is provided by N.S. Currey [18] and based on CG, NLG and MLG relative positions. The value should be as small as possible, not exceeding 63° for a land-based aircraft.

Roll clearance angle
This criterion is a measure of the amount of roll about the MLG (in its most compressed position) available before the deflected control surfaces contact the ground. It should be at least 7.5°, and even higher in the case of engine nacelles located under the wings. The maximum deflection angle for the aps and ailerons are provided by the reports of the GDP wing teams for both aircraft concepts, and the deflected surfaces are implemented in the CAD model to check the roll clearance value. The deflected aileron is the design driver for both the Ae-16 and the A-17.
Using a CAD model featuring the outer surface of the aircraft the longitudinal, lateral, and vertical positions of each landing gear unit can be determined by following all the above constraints. This is the most convenient way to visualize the layout while adjusting the position of the wheels for a given concept, but the adaptation to a different concept is very time consuming and it is difficult to integrate in an optimization framework. Therefore, a MATLAB code was developed in parallel using the same inputs and constraints to obtain the position of the wheels. This secondary method allowed a cross-check of the results and was further developed with every stage of the preliminary design process. A lateral view of the wheels positioning on the Ae-16 is presented in Figure 5. The position results will be used in the following design steps.

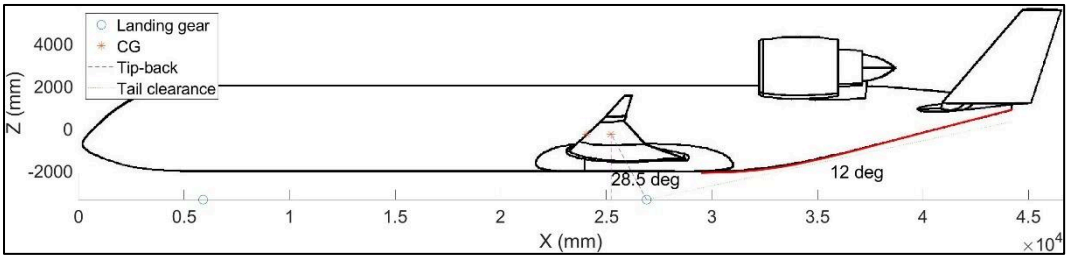


Figure 5. Side view of the wheels position on the Ae-16 generated by the LGPDF showing the tip-back and tail-down angles

2.3.2 Loading actions

The loads applied on the landing system are decomposed in static and landing loads. These values are then used with various coefficients to generate a full list of loading cases acting in every direction, either on the wheel axle or at the ground contact point. All loading actions calculations were done in Excel to facilitate the visualization of parameters variations impact in real time.

Static loads
The static loads are derived directly from the longitudinal position of the ground contact

points. The formulas for the range of loads acting on the main and auxiliary units are listed by N.S. Currey [18] as follows (with the notations from Figure 6, and W the weight of the aircraft):

$$\begin{cases} MLG_{MIN}^{static} = \frac{L}{2*F} * W \\ MLG_{MAX}^{static} = \frac{F-M}{2*F} * W \\ NLG_{MIN}^{static} = \frac{F-N}{F} * W \\ NLG_{MAX}^{static} = \frac{F-L}{F} * W \end{cases} \quad \text{(per strut)}$$

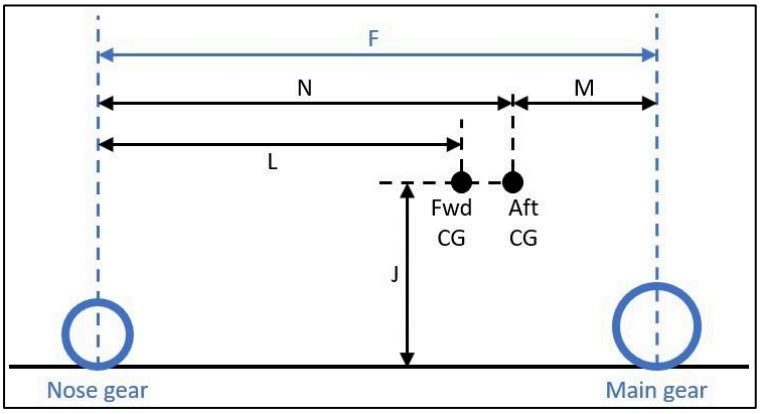


Figure 6. Static loading geometry notations

Typically, the static vertical load on the NLG should be within 5%-14% of the total weight of the aircraft, to ensure maneuverability. "Fwd" and "Aft" respectively refer to the most forward and most rearward positions of the aircraft's center of gravity, depending on the payload distribution.

Landing loads

Three cases are considered, as described by Howe [19]:

- Limit energy condition at the design landing mass, from CS-25 [20]
- Condition at the design take-off mass, from CS-25 [20]
- Ultimate energy condition at the design landing mass

The estimation of the equivalent vertical load on the landing gear R_V comes from the energy balance upon landing. Here we consider the 2-points landing case, where the MLG touches the ground first. The kinetic energy of the aircraft to be absorbed by each MLG unit is:

$$KE_{MLG}^{unit} = \frac{1}{4} * M * V_V^2$$

Then, the energy absorbed by the shock absorber and tires is:

$$E_{ST} = R_V * [\eta_S * \delta_S(R_V) + \eta_T * \delta_T(R_V)]$$

where:

- η_S and η_T are the shock absorber and tire efficiencies with typical values of 0.80 and 0.47 respectively

- $\delta_S(R_V)$ is the wheel vertical axle travel under the vertical load R_V
- $\delta_T(R_V)$ is the tire deflection under the vertical load R_V

At this stage, the load-deflection curves for the shock absorber and tires can be approximated as follows [19]:

$$\begin{cases} R_S = k_S * \delta_S^{0.25} \\ R_T = k_T * \delta_T^{1.1} \end{cases}$$

where:

- k_S is calculated from the value of the total stroke and the ultimate energy case condition
- k_T is calculated using the rated load and loaded radius of the tire.

Conventionally, R_V is determined from the maximum static load R_{stat}^{max} by setting the value of the landing reaction factor λ so that: $R_V = \lambda * R_{stat}^{max}$. Values of λ depend on the type of aircraft and are usually around 1.5 for a medium-sized transport aircraft.
The value of R_V used for the following detailed loading cases is the maximum ultimate value obtained from the three cases described above. This usually originates from the condition at MLM.

CS-25 loading cases
The structural sizing of the landing system is based on a set of applied loads in every direction, given by the airworthiness requirements. Since we are here considering a medium-sized civil transport aircraft, the set of loads will be drawn from the EASA CS-25 documentation [16]. This includes eight cases derived from landing conditions, ten cases derived from ground handling conditions, and a combination of asymmetrical landing and ground handling conditions in the case of multiple wheels units. Since the aircraft configurations (Ae-16 and A-17) di er in several ways which may impact the significance of some loading cases, the choice was made to analyze them all and determine which cases generate critical loads for each direction. This implies that the landing systems may not be sized based on the same set of loading cases for each aircraft concept but will ensure that the actual critical cases will be considered every time.

2.3.3 Tires, wheels and brakes

Tires selection
The dimensions of the tires have an important impact on the volume required to retract and store the landing gear. They must be carefully selected, aiming for minimum weight while being compatible with the applied loads and the infrastructure. Small high-pressure tires are usually applied to fighter aircraft, where stowage volume is more critical than runway impact, but in the case of large airliners it is more common to use larger tires at a lower inflation pressure. This will ensure maximum compatibility with existing airfields.
A wide variety of aircraft tires is available from manufacturers such as Goodyear and Michelin [21,22]. The existing tires properties from all manufacturers are gathered in a common catalog updated yearly by the Tire and Rim Association [23]. Using the maximum static and dynamic load values (on each wheel), an appropriate tire type can be selected from this list, providing all the necessary information on tire (dimensions, rated and maximum loads, rated pressure) and the corresponding wheel rim dimensions.
Here again, to avoid repeating the manual process of selecting a tire from the catalog, the

entire list was transferred into a data file used by a further part of the previously mentioned LGPDF tool. The user inputs the static and maximum dynamic wheel loads and the program generates a short list of suitable tires ranked by total volume, giving the option to choose between high- or low-pressure solutions. Optional parameters are available to reduce the output to a single tire reference.

Flotation analysis

Flotation studies are a way to determine the compatibility of a given aircraft with an airfield, but a wide variety of methods exist because of non-homogeneous soils, the specific problems dealt with by different countries and agencies, economic drivers for pavement construction, and unpaved considerations for military applications. A detailed list of the existing methods for flotation analysis and runway design is given in the AIR 1780A [24], along with a list of recommended documents for both civil and military usage.

To simplify the study of aircraft/airfield compatibility, the International Civil Aviation Organization proposed a uniform methodology based on Aircraft and Pavement Classification Numbers. Although this is not strictly speaking a method for flotation calculations, it is a convenient way to determine whether an aircraft can operate from a given airfield by checking that the ACN is lower than or equal to the PCN. It is however only applicable to flexible and rigid pavements (not applicable to landing mats, membranes, and unsurfaced airfields).

In this study, the ACN values for each landing system are generated using the ICAO-ACN 1.0 software [25]. The values are then compared to similar-sized aircraft to ensure similar airfield compatibility [26].

Wheels and brakes initial sizing

For comparison purposes, all landing system solutions will feature forged aluminum wheels and carbon brakes. Knowing the diameter of the tires and the static wheel load, the weight of each wheel can be estimated using the method presented by N.S. Currey [18].

N.S. Currey also introduced a method for the estimation of brakes dimensions and weight. This initial sizing is done by combining the requirements of the design landing and rejected take-off cases described in Table 1, where V_1 is the take-off decision speed and V_{TD} is the touchdown speed (both speeds were determined by the performance teams of the GDP for each aircraft concept). Initial values are obtained for steel brakes, and conversion factors are used for carbon material results.

Here again, all the charts used to obtain the results were converted in data files and incorporated with the corresponding formulas to another module of the LGPDF. This is for overall flexibility of the global program, as the tires, wheels, and brakes characteristics will not change from one concept to the other (similar aircraft weight and same number of wheels resulting in the same static wheel loading).

Table 1. Brake sizing conditions

Case	Aircraft Mass	Aircraft speed
RTO	MTOM	V_1
DL	MLM	V_{TD}

2.3.4 Shock absorber

Preliminary sizing

The following design method concerns oleo-pneumatic shock absorbers, which are the most

common solutions for current large transport aircraft and will be applied to all the conventional landing system concepts. The first parameter for shock absorber sizing is the stroke, that can be calculated using the maximum VAT value from the landing kinetic energy calculations (see section 2.3.2). In the case of a telescopic strut, the stroke will be approximately equal to the VAT (depending on the rake angle defining the vertical inclination of the strut). In the case of a trailing arm configuration the stroke will depend on the attachment points (on the main strut and lever) and will have to be determined geometrically.
Then, the static characteristics of the shock absorber must be set. These include the static internal pressure, defining the piston diameter, and the static position that can be chosen arbitrarily based on existing aircraft or by setting the amount of remaining volume when the strut is fully compressed [18].
Next, the compression ratios defining the fully extended and fully compressed pressures must be set. For large aircraft, suggested values are [18,27]:

$$\begin{cases} r_{StaticToExtended} = 4 \\ r_{CompressedToStatic} = 3 \end{cases}$$

These parameters can be optimized as described by Kling et al. [13] to reach the minimum shock absorber volume while keeping the extended pressure above 60 psi to allow full extension (avoid internal sticking) and below 300 psi to prevent bouncing upon landing. The fully compressed load should also be consistent with the maximum vertical load determined in the loading actions analysis (see section 2.3.2). The determination of these parameters generated a preliminary load-stroke curve as presented on Figure 7.

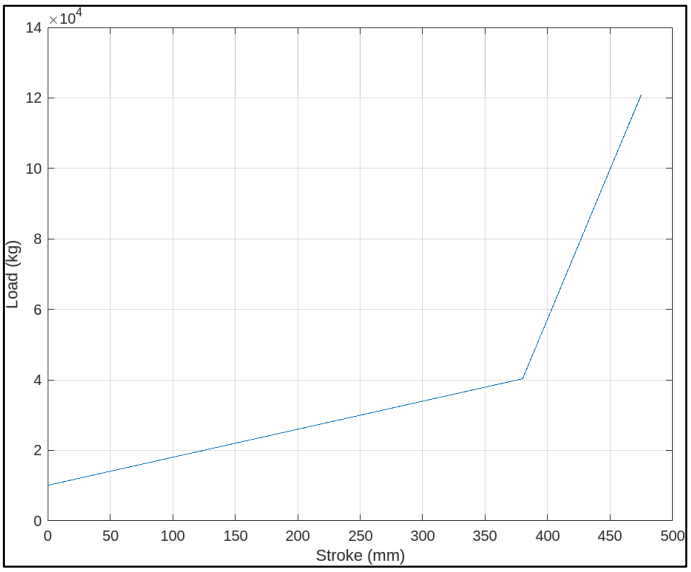


Figure 7. Preliminary shock absorber load-stroke curve example

Detailed load-stroke behavior

The next step of an oleo strut design is the detailed load-stroke curve of the gas spring, based on the universal gas law. To improve shock absorption during taxi phases over rough terrain, this "single-acting" shock strut can be replaced by a "double-acting" one featuring a secondary high-pressure gas chamber that only activates past a certain load.
These considerations on the gas compression lead to more details about the shock absorber behavior, but will not be required for the comparison purposes of this study. Similarly, the

damping characteristics of the shock absorber will not be included in this preliminary design framework as they are part of the detail design of the strut (where internal dimensions are set including the oil orifice diameter) as described by N.S. Currey [18] and will not impact the comparison between the landing system solutions.

Minimum strut length

A final aspect important for the following kinematics studies is to check that there is sufficient length to fit the oleo strut. The minimum strut length must therefore be calculated, and N.S. Currey provides a method for this purpose [18]. The total length of the strut is the addition of the total stroke and the minimum overlap to ensure the stability of the joint between the piston and the cylinder. This minimum overlap is a function of the piston diameter, based on a coefficient depending on the telescopic of trailing arm configuration [28]:

$$\begin{cases} L_{strut}^{min} = S_{total} + k_{ov} * D_{piston} \\ k_{ov} = 2.75\ (telescopic) \\ k_{ov} = 1.25\ (trailing\ arm) \end{cases}$$

2.3.5 Kinematics

The extension and retraction of each landing system solution is studied using CATIA V5 assembly module (see example on Figure 8). This was important to check the feasibility of a given integration configuration, especially in the case of a fuselage-mounted gear. In some cases, a simple inward retraction is not possible, and complexity must be added to the system to enable proper stowage inside the fuselage without adding too much fairing at the expense of aerodynamic performance.

The main constraints to respect concern the attachment points that must be located on existing load-bearing structure, and the clearances between the tires and the inner bay walls. The minimum clearance between a fully grown tire and the surrounding structure is 50 mm. The detailed challenges related to kinematics will be presented with the result of each concept in the following sections, as they are highly dependent on the configuration. On some occasions, the kinematics feasibility required a modification of the initial wheels position (see section 3.1.2 for example), leading to an iteration of the previous steps described and confirming the usefulness of the automation e ort done so far. In such cases, only the final layout will be described in the results and the kinematics drivers will be listed as challenges encountered.

Finally, the feasibility of integrating the necessary actuation power was checked, since the available space around the structure was one of the main anticipated issues of HAR wings.

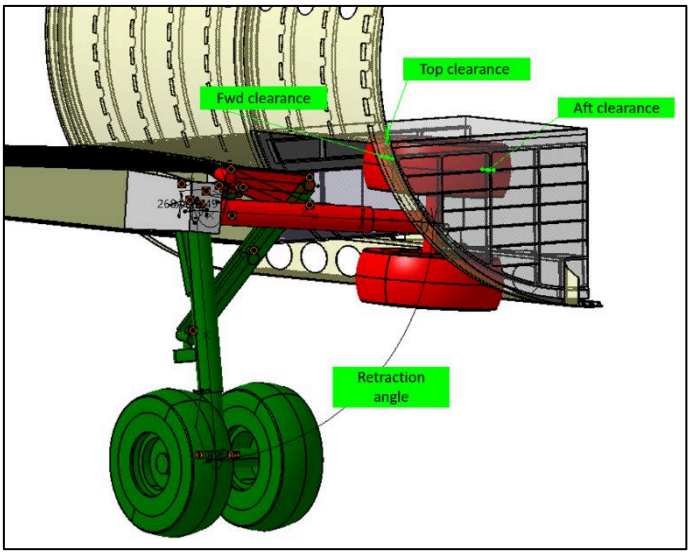


Figure 8. Example of kinematics study on CATIA V5

2.3.6 FEA and structural sizing

Finite elements model

The forces and bending moments in the structural members are obtained by studying all the critical cases from section 2.3.2. For each landing system concept, a rigid beams model is designed and analyzed using MSC NASTRAN/PATRAN. These results will then be used to size the corresponding parts.

The landing gear structure is modeled using rigid beam elements with a uniform circular cross-section. The model does not include the wheels.

The displacement constraints at the attachment points to the airframe are chosen to represent the joint behavior as accurately as possible. The loads are applied to the ends of the wheels' axle, including the torque generated by the o set from the ground contact point when specified in the load-case. Multi-point constraints (MPCs) are used to represent the joints (other than airframe attachments). This allows for a more accurate description of the load path.

The shock absorber is modeled as a linear spring with constant stiffness to obtain a more accurate representation of the displacements than with a fully rigid structure.

An example of the models is presented on Figure 9, featuring the loads and boundary conditions from a simple static load-case.

The generation of the model, the analysis runs, and the extraction of results have all been set up as scripts using the Patran Command Language (PCL). This is done to make the analysis of multiple concepts quicker and easier, as a simple description of the geometry and loads is the only input required by the scripts. The various steps of the analysis (geometry, meshing, loads, boundary conditions, analysis, and results extraction) are kept in individual pieces of code to allow intermediate modifications and maximize flexibility. This was part of the e ort to automate most of the design process, however it would have been more convenient to use a simpler FEA software for the purpose of load-path analysis as no further detailed stress analysis was planned.

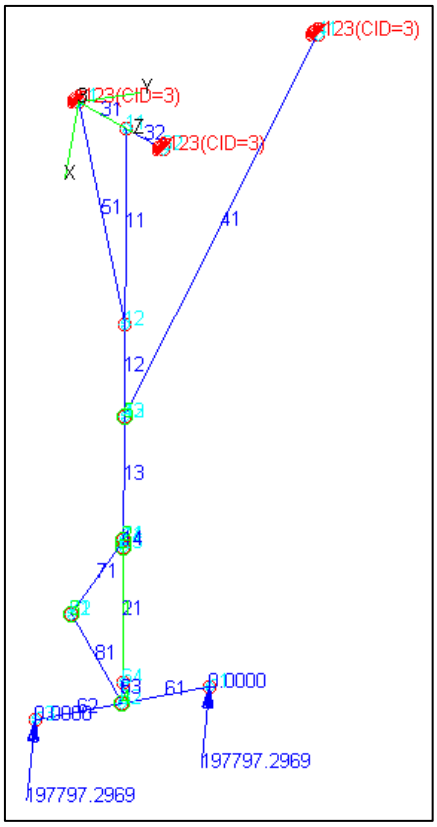


Figure 9. Finite elements model of the landing gear structure

Structural sizing

The final step of the design process for the conventional landing system concepts is the structural sizing of the parts based on the forces and moments obtained from the beams model. This provides an estimation of the structural mass, an important comparison criterion between concepts, and the implementation of the obtained cross-sections in the CAD assembly checks the feasibility of the chosen kinematics concept. For comparison purposes, all structural members will be designed based on 300M steel material properties [29]. Recent progress in high-performance alloys led the development of lighter and even corrosion resistant steels [30], and there is also a trend towards composite materials implementation into landing gear structures [31,32], but these technological advances could potentially improve all the concepts equally and do not bear much value for weight comparisons.

The section of each beam is chosen based on existing similar designs where possible since they went through a much more detailed design process. Alternatively, the choice can be based on the dominant load applied, as described by Weaver [33]. Next, each section's dimensions are optimized using the solver from Microsoft Excel to achieve a minimum Reserve Factor of 1 under each stress condition when submitted to the forces and moments given by the rigid beams model. Internal stresses generated from tension, compression, shear, bending, torsion, as well as buckling considerations are considered for sizing. The maximum values of the loads for each structural element are extracted from the MSC PATRAN report les by an Excel VBA macro, and then used as inputs for each of the section sizing pages on which the Excel solver is based. The detailed formulas used for stress calculations of various sections obtained from various references [34–39]. It is important to note that this is solely a preliminary sizing estimation assuming a constant cross-section along the whole length of each structural

member; to obtain a detailed lighter design, the section should be locally optimized following the shear force and bending moment along the length. This detailed optimization is however outside the scope of the current project.

2.3.7 Weight estimation

The estimation of the wheels and brakes weight is done following the method given by N.S. Currey [18] as previously mentioned. The weight of the tires is estimated from their dimensions (diameter and width) with a statistical formula based on existing tire masses [23,27] as shown on Figure 10.
The structural weight is estimated after the sizing process described in the previous section, using the sized section areas and beam lengths with the assumed material density (300M steel).
To validate the method, the total mass of the main landing gear is compared to an advance statistical estimation formula described by Raymer [40] and detailed with more precise coefficient values by Schmidt [27]:

$$W_{MLG} = 0.09468 * (W_L * N_L)^{0.76802} * \left(\frac{L_m}{12}\right)^{0.40845}$$

where:

- W_{MLG} is the total weight of the MLG (all units) in pounds
- W_L is the maximum landing weight of the aircraft in pounds
- L_m is the extended length of the leg (from the pintle to the wheels' axle) in inches
- N_L is the ultimate landing loading factor (1.5 $*$ reaction factor).

The concept chosen for this validation is the Ae-16 c1 due to its resemblance with an existing Airbus A320 landing gear. The total weight of one MLG unit based on the sizing process features a relative error of $e_{MLG} = 1\%$ compared to the value obtained with the statistical formula. It is important to note that even though this result seems very satisfactory, it remains a rough approximation of the real landing gear weight. The dressing alone (electrical, hydraulic...) would add about 25kg to the overall mass, and many structural elements have been omitted due to the scope of the project (details of joints, lugs, bearings, locks...). On the other hand, the sizing is only preliminary, and a detailed optimization would reduce the structural mass.

2.4 Performance indicator: fuel penalty

The estimation of fuel penalty associated with a landing gear concept is decomposed as follows [41–43]:

- Fuel weight increase due to system weight:

$$(\Delta W_{FO})_{\Delta W_A} = \Delta W_A * \left(e^{\frac{c*t*g}{r}} - 1\right)$$

- Fuel weight increase due to system drag:

$$(\Delta W_{FO})_{\Delta D} = r * \Delta D * \left(e^{\frac{c*t*g}{r}} - 1\right)$$

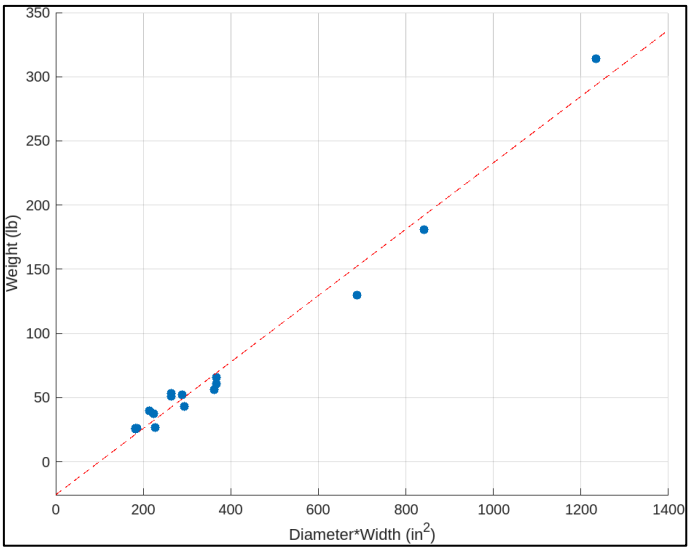


Figure 10. Correlation between dimensions and weight for aircraft tires

The fuel penalty due to system power off-take is not included in the scope of this study, as no data was generated during the preliminary sizing to allow for a comparison of the concepts. The estimation of the drag characteristics is based on the project specifications of each aircraft. The detailed design and CFD analysis of the fuselage additional belly fairing being out of the scope of this project, the comparison will take place between the concepts that require streamlined fairing and the ones that can be fully stored within the initial fuselage cross-section. This will impact the value of the zero-lift drag coefficient C_{D0} that will be approximated using a formula from Torenbeek [42]:

$$C_{D_0} = r_{Re} * r_{LG} * \left[r_t * \left\{(C_D S)_W + (C_D S)_f\right\} + (C_D S)_n\right]$$

where:

- $(C_D S)_W$ is the uncorrected drag area for smooth wings
- $(C_D S)_f$ is the uncorrected parasite drag for streamlined shapes (fuselage)
- $(C_D S)_n$ is the uncorrected nacelle drag
- r_{Re} is the correction factor for Reynolds number and miscellaneous drag
- r_{LG} is the drag penalty from the landing gear
- r_t is the tail plane drag factor

All of these parameters will be considered constant for all concepts, except for the landing gear drag penalty factor r_{LG} (see Table 2). The drag estimation results will then be converted into fuel penalty, and the total fuel penalty will be the nal key performance indicator to compare the landing system solutions.
It is important to note that this may not accurately represent the variation of drag due to the landing system alone as some fairing is usually added around the wing-fuselage interface to reduce interference drag even if the wheels t fully within the fuselage initial cross-section.

Table 2. Drag penalty factor for various landing gear configurations [42]

Configuration	**r_LG**
Fully retracted within the aircraft's external lines	1.00

Main gear retracted in nacelles or turboprop engines	1.03
Main gear retracted in streamlined fairings on the fuselage	1.08
Fixed gear with streamlined wheel fairings and struts	1.25
Fixed gear without streamlined wheel fairings	1.35

3 Results and discussions

3.1 Ae-16: Low-mounted HAR wing aircraft

3.1.1 Integration challenges for the wing mounted landing gear

General description

As previously described, the baseline landing system for this aircraft configuration is adapted from the Airbus A320 layout. The main landing gear is composed of two pairs of twin wheels connected to the inner wing by a telescopic strut. The main wheels retract inward into the fuselage belly fairing. This concept will be referred to as *"Ae-16 c1"* in the following.
The attachment points and kinematics of this concept are directly inspired by the Airbus A320 landing gear and are shown in Figure 8. The main fitting is attached aft of the wing's rear spar, with an added supporting structure reproducing the idea of the "false" rear spar. The side-stay is attached to the fuselage reinforced frame supporting the aft part of the wing box. The landing gear retracts inwards inside the fuselage, with a small rearward angle to prevent an interface issue between the tires and the wing-box structure. The side-stay is divided into two beams linked by a pivot joint, and folds in front of the main strut upon retraction. Unlike the A320 design, no universal joint was required to allow for rotation about the side-stay direction as all members fold within the same plane. This increases the simplicity of the assembly.

Retraction angle

The retraction angle of the main strut is $\alpha_{retraction} = 83$ to ensure sufficient clearance with the top bulkhead, meaning that the wheels are not horizontal when retracted. This is sub-optimal in terms of storage volume, however the short height of the HAR wing does not allow to position the pintle attachment point low enough to retract at 90 with the selected wheels spacing. Apart from the internal clearances when stored, the distance between the tires and the keel beam must be checked during the extension/retraction process. This is achieved using the DMU Kinematics module from CATIA V5, and the minimum distance is above the $50mm$ allowable clearance, which is satisfactory.

Wing integration

An important issue that was noticed during integration and sizing is the available space for the pintle supporting the main strut. Ideally, it should be about one third of the total length of the strut (as per Airbus A320 design) which would clearly not t within the space aft of the rear spar. However, the supporting structure of the pintle is derived from the Advanced Low Cost Aircraft Structures project that demonstrated the feasibility of a composite structural part transmitting the loads from the pintle to the wing [44].
The loads acting on the pintle obtained through FEA are smaller than the ones used to design the structure of the ALCAS project, which shows that the limited length of the pintle will not be an issue for our HAR wing geometry. However, should the root chord be reduced any further, it may become necessary to implement a dual side-stay to distribute the loads into the fuselage as it is done on the Airbus A350 for example.

3.1.2 Integration challenges for the fuselage mounted landing gear

General description

The second concept applied to the Ae-16 aircraft is a fuselage integrated landing gear, with a trailing arm shock absorber configuration similar to the BAe 146 design [45]. This option is described as an alternative to the telescopic fuselage landing gear studied by Kling et al. for a HAR wing aircraft with aircraft positioned over the wings [13]. This concept will be referred to as *"Ae-16 c2"* in the following.

The main landing gear is a trailing arm configuration, attached to the lower part of the fuselage and the wing-box. The main strut and drag-stay are attached to heavy frames just behind the wing-box, and pivot about an axis parallel to fuselage to retract inward (see Figure 11). The trailing arm is attached at the bottom of the main strut, and pivots in the vertical plane to absorb vertical loads and shorten upon retraction. The shock absorber is attached to the trailing arm and to a shortening connector pivoting about the main strut along the aircraft longitudinal axis upon retraction. The extension/retraction kinematics with intermediate positions are shown on Figure 12, illustrating the "stick diagrams" that were used to adjust the multiple geometrical parameters (attachment point, strut length, trailing arm retraction angle...) and obtain an optimal retracted position with minimal clearances to the bay walls.

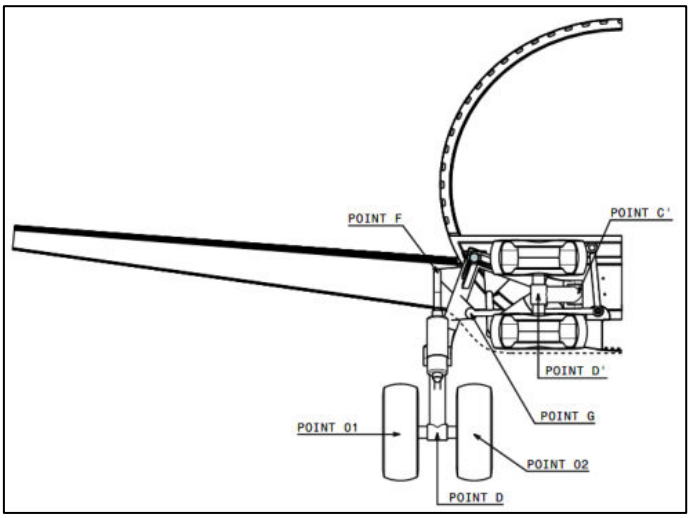


Figure 11. Ae-16 c2 retraction (front view)

Initial interface issues

The stick diagrams highlighted multiple integration issues and led to several design changes before obtaining the final configuration. The initial track value (kept from Ae-16 c1) and static ground line set for a tail-down angle of $\alpha_{TD}^{init} = 12°$ generated an overlap between the main strut and the fuselage center line upon retraction. Keeping the same tail-down angle, the issue was solved by slightly reducing the track value. This choice reduced the roll clearance angle, while keeping it at a reasonable value (above 7.5°) thanks to the engines being located off the wings.

The next issue was the longitudinal position of the wheels in static position. As it was initially set to the same value as Ae-16 c1 for comparison purposes, the wheels were located almost directly below the rear spar which was not compatible with the trailing arm configuration. The initial idea was to modify the concept chosen during the first phase of the project (see section

2.2) and switch back to a telescopic strut attached to the fuselage, as it was done by Kling et al. [13]. However, due to the tail-down angle requirements and the fuselage geometry of the Ae-16, this led to a considerable overlap of the fuselage center line upon retraction. The necessary retraction axis angle to clear the center line resulted in a rearward retraction that would considerably lengthen the storage space and required an emergency extension solution other than free-fall. This solution was discarded, and another workaround was agreed with SLS experts: incline the main strut forward to the maximum angle allowing wing-box clearance upon retraction and shift the longitudinal position of the MLG wheels aft. This led to an increase of the NLG static load range to 11-17%, and a landing gear bay length increase to the aft for tire clearance (much smaller than for the rearward retraction of a telescopic strut), which was deemed satisfactory.

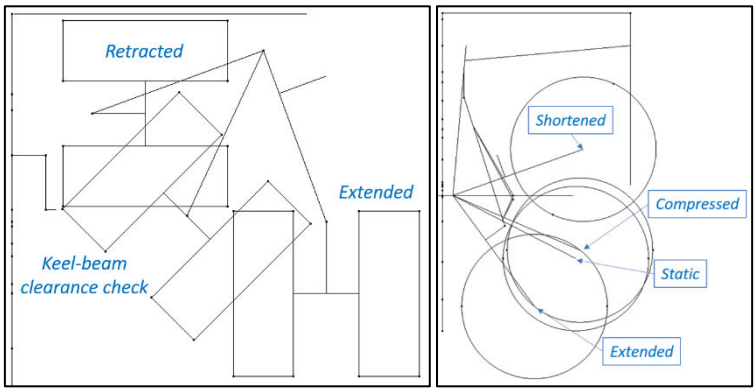


Figure 12. Ae-16 c2 kinematics front and side views

Shortening mechanism

The top part of the shock absorber cylinder is attached to a "shortening connector" that rotates outward to raise the trailing arm and shorten the overall assembly upon retraction. The design of this shortening connector is constrained by three trailing arm positional requirements (two of which are shown on Figure 12):

- The extended angle (below horizontal)
- The fully retracted angle (above horizontal)
- An intermediate angle for keel beam clearance

Each of these positions corresponds to an angle of the shortening connector in the front plane, controlled throughout the retraction process by a direction rod attached to the fuselage with a pivot joint and to the connector through a short crank (see Figure 13). The dimensions of the crank and rod as well as the rod-fuselage hinge position are determined using the three angle requirements for the trailing arm position, resulting in satisfactory clearance values. The integration of the actuator was not studied in detail as it did not represent a particular challenge for this configuration. It is possible to simply adapt the pulling actuator from the existing BAe 146 concept.

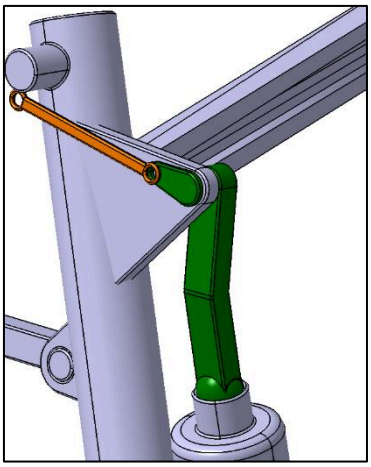


Figure 13. Ae-16 c2 shortening mechanism with connector-crank (green) and direction rod (orange)

3.1.3 Performance comparison of the solutions

The low-mounted HAR wing generated various challenges for each of the studied configurations. The wing-mounted telescopic strut (c1) leads to a sub-optimal retraction angle from a storage point of view and there is very limited space for the pintle support structure. Both issues show the limits arising from the short root chord and slenderness of the HAR wing: should the wings dimensions be reduced any further there is a high risk that this solution will not be compatible with the airframe, driving towards an alternative (fuselage-mounted) concept.

The fuselage-mounted trailing arm (c2) leads to longitudinal position constraints increasing the load on the NLG to critical values and requires a longer storage bay, impacting the cargo capacity. These issues show the limited compatibility between low wings and fuselage gear, that could become very challenging depending on the CG range. Looking at the trend towards hydrogen-fueled aircraft such as the Airbus ZEROe concepts [46], the integration of an aft-fuselage tank would likely shift the CG range rearward which would act in favor of this landing system solution. It is also a much more complex assembly that is likely to raise the maintenance costs, and a heavier system.

From a fuel penalty point of view, the system weight is the only contributor as both concepts require a streamlined fairing to be stored. The normalized results representing the relative difference between the concepts are included in Figure 14, and Figure 15 illustrates the advantages (green) and disadvantages (red) of each concept over the other. The drag penalty remains neutral (yellow) for both as previously mentioned.

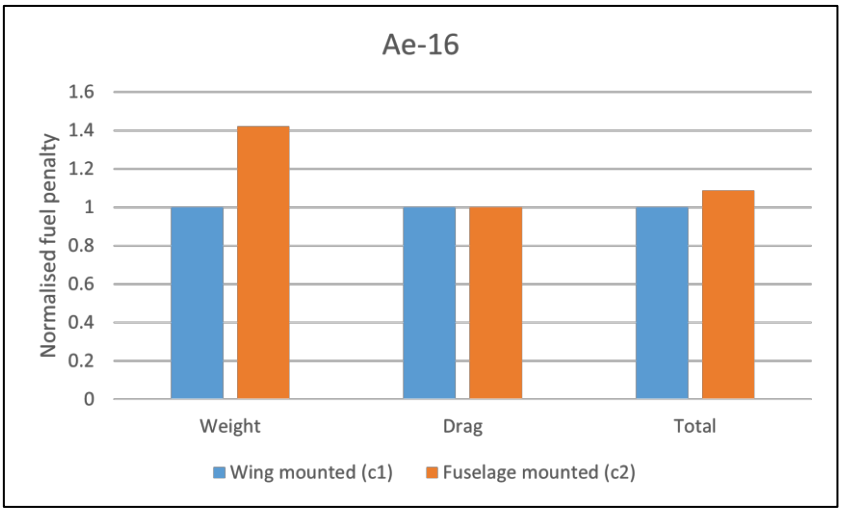


Figure 14. Normalized fuel penalties for Ae-16 c1 and c2

Criteria	C1	C2
Simplicity	✓	✗
Cargo space	✓	✗
Weight	✓	✗
Drag	–	–
Fuel penalty	✓	✗

✓ → *better*
✗ → *worse*
– → *equivalent*

Figure 15. Comparison summary of Ae-16 c1 and c2

Overall, the wing-mounted concept (c1) is a better solution as long as it remains compatible with the wing dimensions. Should the fuselage mounted gear be necessary, an investigation into composite materials could potentially mitigate the weight penalty of the design. The number of structural parts is higher, but they are more simply loaded which facilitates the implementation of composite structures and this technology has already been implemented on landing gear parts [31,32,47,48]. Alternatively, it would be interesting to investigate unconventional landing system solutions that could potentially mitigate the issues of both conventional concepts.

3.2 A-17: High-mounted UHAR wing aircraft

3.2.1 Integration challenges for the trailing arm landing gear

General description

The first concept applied to the A-17 aircraft is a fuselage-mounted landing gear similar to the second concept of the Ae-16. The main landing gear is a trailing arm configuration, attached to the lower part of the fuselage structure (see Figure 16). The main strut and drag-stay are attached to heavy frames, aft of the wing-supporting struts, and pivot about an axis parallel to fuselage to retract inward. The trailing arm is attached at the bottom of the main strut, and pivots in the vertical plane to absorb vertical loads and shorten upon retraction. The shock absorber is attached to the trailing arm and to a shortening connector pivoting about the main strut along the aircraft longitudinal axis upon retraction. Here again, the retracted position was determined using "stick diagrams" as shown on Figure 12. This concept will be referred to as *"A-17 c1"* in the following.

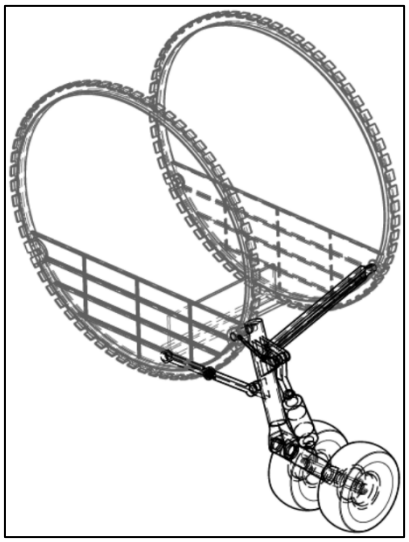


Figure 16. A-17 c1 structural environment (isometric view)

Initial interface issues

Just like Ae-16 c2, this concept required a reduction of track and height values which impacted the ground stability characteristics and drove the tail-down angle value to its minimum allowable value (according to the aircraft's performance data). Therefore, any attempt to lengthen the fuselage in the context of an aircraft family expansion would require re-designing the landing system. A similar issue was encountered by Boeing when designing the 737 MAX 10 and solved by adding a spring-loaded lever to extend the telescoping landing gear, plus a "shrink link" mechanism that pulls the extension inward when it needs to be folded back up [49].

The second issue originated from the vertical axle travel value initially set to match the Airbus A320 touchdown performance, and the original longitudinal position of the attachment point (first fuselage frame aft of the wing struts). This led to a very high angle between the main strut and the trailing arm in the fully extended position, compromising the shock absorber integration and performance. The selected workaround was to relocate the front attachment point of the main strut and attach it to the heavy frame supporting the wing struts. This allowed to keep the wheels position and loads distribution while sufficiently lengthening the trailing arm to solve the extended angle issue.

Wings-struts structural overlap

The new position of the main strut clashed with the wing-supporting struts; however, it did not interfere with the actual structure but only with the fairing surrounding it (as shown on Figure 17). This was deemed satisfactory as the fairing can be adapted without causing major changes to the airframe load-bearing structure. These decisions defined the final positions of the wheels and attachment points, together with the strut and trailing arm geometries.

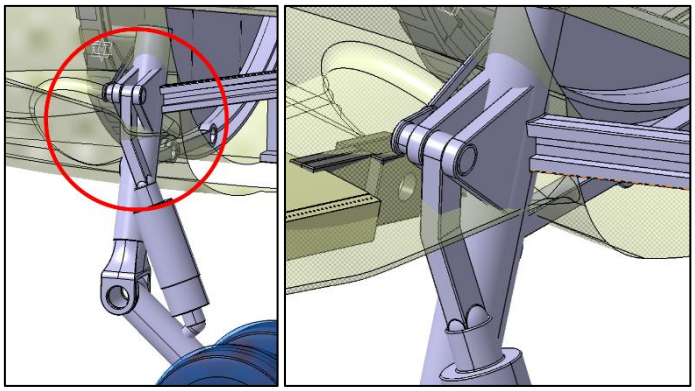


Figure 17. A-17 c1 interface issue with wing struts

Shock absorber integration

After freezing the main strut and trailing arm design, the shock absorber can be integrated. This required choosing the location of the attachment points on the strut and trailing arm, which will affect the load and stroke of the shock absorber, as well as the shortening system design. A first study is conducted on the effective lever ratio R_L^{eff} linking the shock absorber load to the wheel axle load: $F_{SA} = R_L^{eff} * F_{axle}$. This value has a direct impact on the shock absorber length as shown on Figure 18, and it can be chosen as a design parameter to minimize the dimensions and ease storage. These results are then combined with CAD modeling to check that enough space will be provided between the strut and trailing arm attachments, while allowing the shortening system to raise the trailing arm to its fully retracted position. If the strut attachment point is too low, the shortening connector becomes too short to allow full retraction. Finally, the shortening mechanism is designed and integrated in the same way as for Ae-16 c2 (see Section 3.1.2).

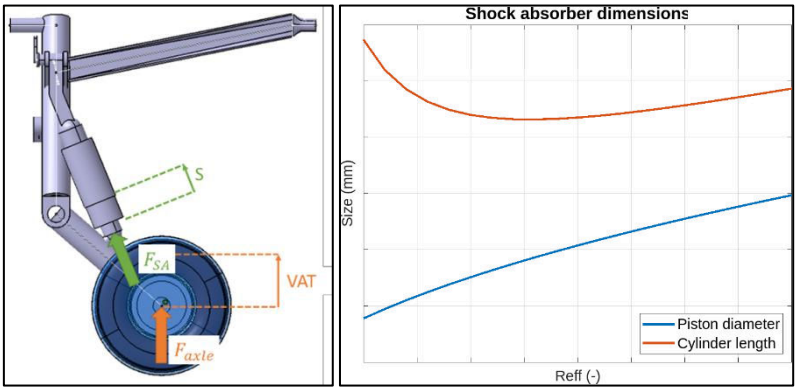


Figure 18. A-17 c1 shock absorber effective lever ratio

3.2.2 Integration challenges for the telescopic landing gear

General description

The main landing gear is a telescopic tandem-wheels configuration attached to the lower part of the fuselage structure (see Figure 19), inspired by the design of Obrovsky [50]. The main strut and side-stay are attached below the cabin floor structure, and pivot to retract rearward into the fuselage. The bogies beam supporting the wheels is attached at the bottom of the piston and pivots about two axes (longitudinal and transverse) to keep the wheels horizontal upon retraction and tilt them to t the fuselage cross-section curvature. The

extension/retraction kinematics with intermediate positions are shown on Figure 20, illustrating the "stick diagrams" that were used to adjust the multiple geometrical parameters (attachment point, strut angle to vertical, all retraction angles) and obtain a satisfactory retracted position with the wheels fitted inside the fuselage structure. This concept will be referred to as *"A-17 c2"* in the following.

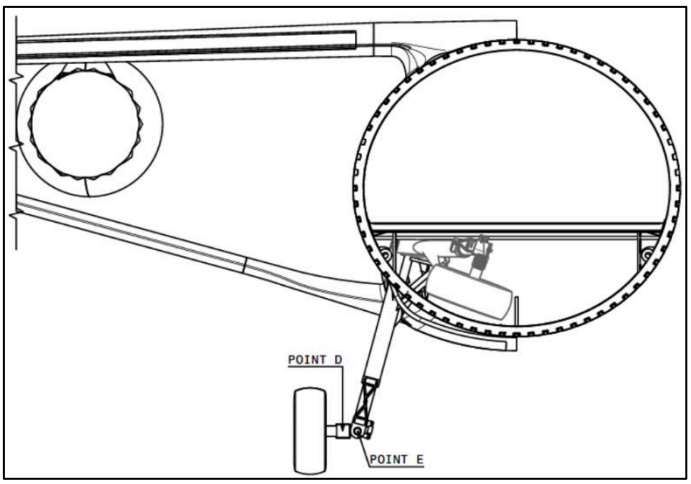


Figure 19. A-17 c2 retraction (front view)

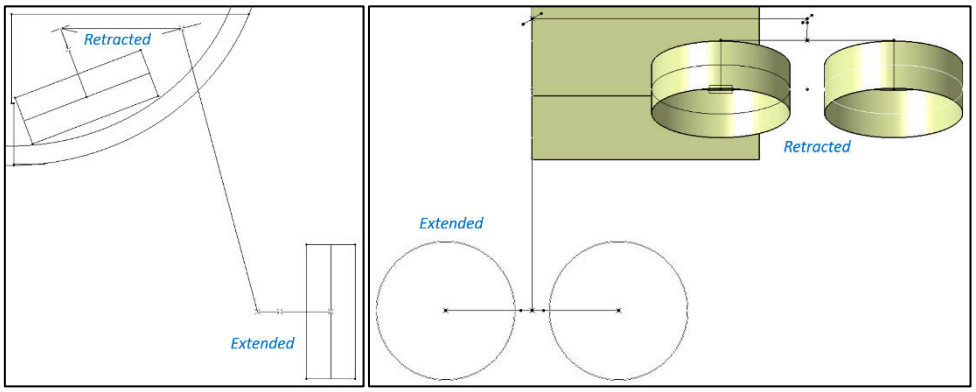


Figure 20. A-17 c2 kinematics front and side views

Integration issues

The first issue arising from the fuselage mounted telescopic configuration is the main strut angle to vertical (around the fuselage longitudinal axis). This angle causes a reduction in track as the shock absorber is compressed, impacting stability. Moreover, it reduces the shock absorber performance which is designed to be axially compressed. The strut angle around the aircraft's longitudinal axis α_{strut} was set to t the track requirements for ground stability with the given fuselage geometry.

Then, due to the presence of the wing-supporting struts, a forward retraction similar to the BAC TSR-2 concept was not possible, and a rearward retraction had to be implemented. This will require the use of a separate emergency extension system that can be of various nature [51]: cable linkage and actuator bypass valve, electric explosion (used on UAVs and small aircraft), electro-hydraulic actuator (as on Boeing 787), or electro-mechanical actuator (as on Airbus A380). This additional system will add weight and complexity to the overall assembly. Furthermore, unlike the inward retraction of A-17 c1, the rearward retraction will

induce a shift in CG position that will need to be carefully monitored during take-off and landing phases.
Next, all the rotation angles required to fully retract the wheels inside the fuselage were determined. This was done combining the stick diagrams shown on Figure 20 with a simple version of the assembly using un-sized parts. Unlike the shortening of A-17 c1 that was mechanically coupled to the main retraction actuator, all these rotations must be actuated separately. This significantly increases the complexity of the assembly and the associated maintenance costs. The resulting retracted position removes the need for additional belly fairing which improves the drag performance of the aircraft, but also requires to lengthen the storage bay which reduces the cargo capacity (see Figure 21).

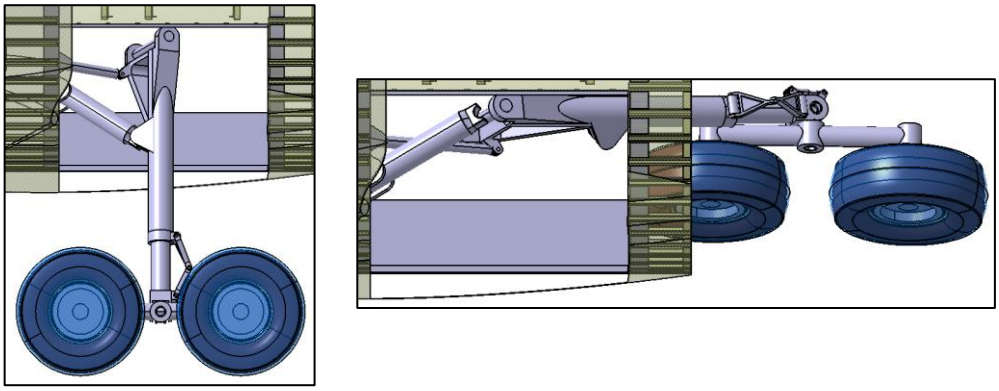


Figure 21. A-17 c2 extended and retracted side view

The final issue to solve was the integration of the drag-stay to the overall retraction kinematics. The first option was to integrate a folding drag-stay behind the main strut, but the floor structure did not leave sufficient space for retraction and led to an interface issue affecting the cabin. The second idea was to implement a telescopic drag-stay in front of the main strut, similar to the outrigger design of the BAe Harrier [52], but this led to an attachment point located outside of the fuselage section due to the main strut rotation axis position. Moreover, it raised safety issues linked to the high drag loads acting on braked wheels, unlike the BAe Harrier outriggers that were un-braked wheels. The final solution chosen was the use of a separate drag-stay that engaged with the main strut upon extension, acting as a down-lock mechanism. This is similar to the design choice of F. Obrovsky [50] but requires an additional mechanism to ensure its retraction inside the fuselage once separated from the main strut, thus adding further complexity to the design.

3.2.3 Performance comparison of the solutions

The high-mounted strut-braced UHAR wing generated various challenges for each of the studied configurations. The trailing arm concept (c1) leads to borderline ground stability characteristics and a low tail-down angle that will not enable a version of the plane with a longer aft fuselage. Improving on these parameters would generate multiple interface issues and require an even more complex retraction mechanism. Moreover, the wing-strut structure generates further integration constraints and could make the integration impossible should the CG range move forward. It does however bene t from the mechanical coupling of the shortening mechanism, preventing the addition of a secondary actuator that would increase complexity and maintenance cost.
The telescopic tandem wheels concept (c2) features much more complex kinematics requiring

four separate actuation systems (main strut, bogie pitch, bogie tilt, and cylinder rotation) and an additional emergency extension device. The angle of the main strut to vertical reduces the shock absorber performance. All of these items reduce the reliability of the overall assembly and increase the maintenance cost. Moreover, it requires a much longer storage bay, impacting the cargo capacity of the aircraft. It does however t entirely within the fuselage structure, removing the need for additional belly fairing and improving the drag performance of the aircraft. From a weight point of view, it is equivalent to the trailing arm (c1).
Therefore, the difference in fuel penalty mainly comes from the removal of the additional fairing. The normalized results representing the relative difference between the concepts are included in Figure 22, and Figure 23 illustrates the advantages (green) and disadvantages (red) of each concept over the other.

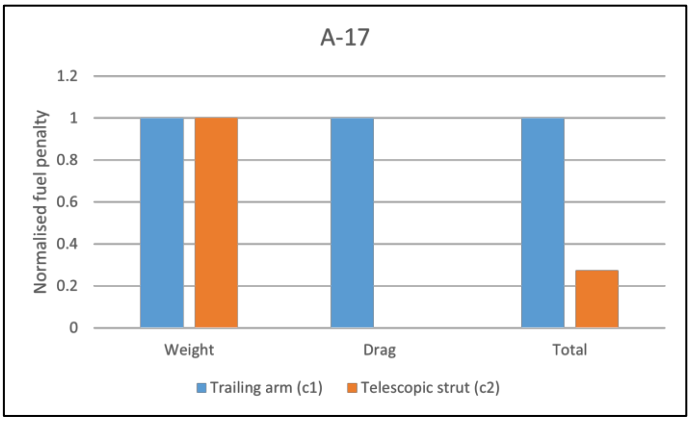


Figure 22. Normalized fuel penalties for A-17 c1 and c2

Criteria	C1	C2
Simplicity	✓	✗
Cargo space	✓	✗
Weight	✓	✗
Drag	✗	✓
Fuel penalty	✗	✓

✓ → better
✗ → worse
▭ → equivalent

Figure 23. Comparison summary of A-17 c1 and c2

Overall and despite its complexity, the telescopic tandem concept (c2) appears to be a more efficient solution for this aircraft configuration. The drag reduction from the removal of the belly fairing generates considerable fuel savings for a given range, but a more detailed study of the implications of the system's complexity on weight penalty, power off-take, and maintenance costs would be necessary to ensure its cost effectiveness. Moreover, a similar arrangement was fitted on the canceled BAC TSR-2 program and raised a number of issues leading Sir Frederick Page (head of the English Electric team on TSR-2) to say that "to avoid trouble in service the undercarriage should have been a rigid leg levered suspension design" [53]. This supports the investigation into unconventional landing system solutions for this type of aircraft.

3.3 Limitations of results and future work

The methodology for landing system grading and ranking and the subset of solutions that emerged from its application were somewhat subjective. The scores attributed to each category for a given solution were qualitative estimations based on experience, and it would be interesting to analyze more concepts in detail to cross check the performance rankings. However, this would require further automation of the analysis framework to process more concepts within the allocated time which was out of the scope of this project.
Moreover, due to time limitations and the high number of studies to conduct, only top-level analyses were achieved, and the performance indicators should be refined to allow an accurate comparison of the different solutions. The impact of each landing system configuration on the weight of the supporting airframe was not considered in the fuel penalty calculations even though important changes to the wing and fuselage structure may be required. The drag analysis used to calculate the total fuel penalty induced by a given concept is a very rough approximation, and the level of detail achieved for the design and integration of the landing system could allow a much more accurate comparison by integrating a CFD solver with simplified geometries in the overall analysis framework.
Furthermore, the inclusion of system safety considerations in the analysis framework would be an interesting area to investigate as future work because it could result in the identification of additional challenges and necessary technologies.
Finally, cross-referencing the findings with existing studies based on objective analysis (or other approaches) could prove beneficial to ensure the robustness of the selected method.

4 Conclusions

The urgency of climate change has imposed strict environmental constraints across all industries to reduce greenhouse gas emissions quickly. The aerospace sector aims to cut CO2 emissions by 50% by 2050 from 2005 levels. Achieving this target requires developing disruptive aircraft designs by 2035, as incremental improvements are insufficient. These new aircraft will likely feature high aspect ratio wings, incompatible with conventional landing systems.
This research studied various landing system solutions for novel aircraft designs. Two potential future aircraft concepts were selected from Cranfield's MSc group design projects for detailed analysis. These included a low-mounted high aspect ratio wing hybrid airliner (Ae-16) and a high-mounted ultra-high aspect ratio wing airliner (A-17), both designed as single-aisle medium-range airliners with similar specifications.
Twenty landing system solutions were initially identified for each aircraft, eventually narrowing down to two for each through a decision-matrix method. The studies showed that the Ae-16's wing slenderness led to storage and structural challenges, suggesting a fuselage-mounted gear could be easier to integrate for even more slender wings. However, this raised concerns about weight distribution and nose gear design. For the A-17, high-mounted wings caused stability and clearance issues. Switching from a trailing arm to a telescopic arrangement added complexity.
Performance assessments revealed that wing- and fuselage-mounted solutions differed mainly in weight for the Ae-16. Although the wing gear was viable, a fuselage-mounted gear's increased weight might be offset by using composite materials. For the A-17, both trailing arm and telescopic concepts had similar weights, but the telescopic strut's integration within the fuselage posed fewer drag penalties, despite its complexity.

Both conventional solutions faced significant challenges, indicating the need to explore unconventional concepts for simplicity and weight reduction.

References

1. King AD., Karoly DJ. Climate extremes in Europe at 1.5 and 2 degrees of global warming. Environmental Research Letters. 2017; 12(11). Available at: DOI:10.1088/1748-9326/aa8e2c

2. Levin K. Half a Degree and a World Apart: The Difference in Climate Impacts Between 1.5C and 2C of Warming. World Resources Institute. 2018. Available at: https://www.wri.org/insights/half-degree-and-world-apart-difference-climate-impacts-between-15c-and-2c-warming

3. United Nations. Summary of the Paris Agreement. United Nations Framework Convention on Climate Change. 2015; : 27–52. Available at: http://bigpicture.unfccc.int/#content-the-paris-agreemen

4. Rogelj J., Shindell D., Jiang K., Fifita S., Forster P., Ginzburg V., et al. Mitigation Pathways Compatible with 1.5°C in the Context of Sustainable Development. IPCC special report Global Warming of 1.5 °C. 2018; : 82pp. Available at: https://www.ipcc.ch/site/assets/uploads/sites/2/2019/02/SR15_Chapter2_Low_Res.pdf

5. Air Transport Action Group. Facts & figures. 2020. Available at: https://www.atag.org/facts-figures.html (Accessed: 29 July 2021)

6. IATA. Aviation & Climate Change - Fact Sheet. 2021; 2025(July): 1–2.

7. IATA. Aircraft Technology Roadmap to 2050. 2019. Available at: https://www.iata.org/en/publications/technology-roadmap/

8. Mistry S., Smith H., Fielding JP. Development of novel aircraft concepts to reduce noise and global warming effects. Collection of Technical Papers - 7th AIAA Aviation Technology, Integration, and Operations Conference. 2007; 1(September): 593–601. Available at: DOI:10.2514/6.2007-7753

9. Mistry S., Smith H., Fielding JP. Novel design concepts for aircraft with reduced noise and global warming characteristics. ICAS Secretariat - 26th Congress of International Council of the Aeronautical Sciences 2008, ICAS 2008. 2008; 2(X): 3408–3414.

10. Willie B. Analytical Weight Estimation of Unconventional Landing Gear. 48th Annual Conference, Alexandria, Virginia, May 22-24. Alexandria, Virginia: Society of Allied Weight Engineers, Inc.; 1989. p. 15. Available at: https://www.sawe.org/papers/1905/buy

11. Cumnuantip S. Landing gear positioning and structural mass optimization for a large blended wing body aircraft. DLR Deutsches Zentrum fur Luft- und Raumfahrt e.V. - Forschungsberichte. 2014. pp. 1–139. Available at: https://www.scopus.com/inward/record.uri?eid=2-s2.0-84905457246&partnerID=40&md5=8aa4d8d19c1ef746d0777dfed5d284f0

12. Nuti A., Bertini F., Cipolla V., Di Rito G. Design of a Fuselage-Mounted Main Landing Gear of a Medium-Size Civil Transport Aircraft. Aerotecnica Missili & Spazio. 2018; 97(2): 85–95. Available at: DOI:10.1007/bf03405803

13. Kling U., Brügge T., Peter F., Hornung M. A framework for unconventional landing gear configuration modelling. 31st Congress of the International Council of the Aeronautical Sciences, ICAS 2018. 2018. Available at: https://www.icas.org/ICAS_ARCHIVE/ICAS2018/data/papers/ICAS2018_0688_paper.pdf

14. Kling U., Hornung M. Landing Gear Integration into Aircraft Structure in Early Design Stage. 2019. Available at: DOI:10.4271/2019-01-1890

15. Ma Y., Abouhamzeh M., Elham A. Aerostructural Optimization and Comparative Study of Twin-Fuselage and Strut-Braced-Wing Aircraft Configurations. Journal of Aircraft. May 2024; 61(3): 839–856. Available at: DOI:10.2514/1.C037388

16. Ilic C., Wegener P., Ruberte Bailo J., Himisch J., Geisbauer S., Wunderlich T., et al. Phased High-Fidelity Aerodynamic Design From Scratch of a Very High-Aspect Ratio Narrow-Body Airliner. AIAA AVIATION FORUM AND ASCEND 2024. Reston, Virginia: American Institute of Aeronautics and Astronautics; 2024. Available at: DOI:10.2514/6.2024-3838

17. Cranfield University. Aerospace Vehicle Design MSc. Available at: https://www.cranfield.ac.uk/courses/taught/aerospace-vehicle-design (Accessed: 1 December 2024)

18. Currey NS. Aircraft landing gear design: principles and practices. American Institute of Aeronautics and Astronautics; 1988.

19. Howe D. Aircraft loading and structural layout. London Professional Engineering Publishing Limited; 2004. 591 p.

20. EASA. Certification Specifications and Acceptable Means of Compliance for Large Aeroplanes CS-25 Amendment 22. 2018. Available at: https://www.easa.europa.eu/document-library/certification-specifications/cs-25-amendment-22

21. Goodyear tire and rubber company. Global Aviation Tyres Databook. 2018.

22. Michelin. Which Michelin® tire is right for you aircraft? Commercial and regional segment. 2020. Available at: https://aircraft.michelin.com/wp-content/uploads/sites/15/2020/10/DataSheets-–-ComReg-October-update.pdf

23. Tire and Rim Association. Aircraft year book. Akron, Ohio: Tire and Rim Association; 2021. 92 p. Available at: https://us-tra.org/publications.html

24. SAE A-5B Gears Struts and Couplings Committee. AIR1780A - Aircraft Flotation Analysis. SAE International; 2021. Available at: https://saemobilus.sae.org/content/AIR1780A/

25. Brill DR. ICAO-ACN 1.0. Federal Aviation Administration. 2015. Available at: https://www.airporttech.tc.faa.gov/Products/Airport-Safety-Papers-Publications/Airport-Safety-Detail/ArtMID/3682/ArticleID/9/ICAO-ACN-10

26. Transport Canada. Aircraft Classification Numbers (ACN's). 2004; (June 2004): 1–19. Available at: https://www.eddh.de/x-files/dl_files/acn-tables.pdf

27. Schmidt RK. The Design of Aircraft Landing Gear. SAE International; 2021. 1090 p. Available at: https://www.sae.org/publications/books/content/r-455/

28. US Air Force. Military Specification - Landing Gear, Aircraft Shock Absorber (air-oil type). 1965. Available at: http://everyspec.com/MIL-SPECS/MIL-SPECS-MIL-L/MIL-L-8552C_8558/

29. Niu MC-Y. Airframe Structural Design - Practical Design Information and Data on Aircraft Structures (2nd Edition). AD Adaso/Adastra Engineering LLC; 1999. Available at: https://app.knovel.com/hotlink/toc/id:kpASDPDID1/airframe-structural-design/airframe-structural-design

30. Aubert & Duval. Sustainable solutions for aerospace high integrity components. 2019. Available at: https://www.aubertduval.com/wp-media/uploads/2019/06/Aeronautical-brochure-BD.pdf

31. Dr. Dell'Anno G., Prof. Partridge IK., Dr. Cartie DDR., Prof. Tatam RP., Prof. Pickett AK., Dr. Skordos AA. Composite landing gear brace for Boeing 787 Dreamliner – first in the market for Messier-Bugatti-Dowty. 2014. Available at: https://impact.ref.ac.uk/casestudies/CaseStudy.aspx?Id=17852

32. Safran. Boeing 787: composites make a successful landing | Safran. 2013. Available at: https://www.safran-group.com/media/20100903_boeing-787-composites-make-successful-landing (Accessed: 27 September 2020)

33. Weaver PM., Ashby MF. Material limits for shape efficiency. Progress in Materials Science. 1998; 41(12): 61–128. Available at: DOI:10.1016/s0079-6425(97)10034-2

34. ESDU 71005. Buckling of flat plates in shear. Engineering Sciences Data Unit; 1995. Available at: https://www.esdu.com/cgi-bin/ps.pl?sess=cranfield5_1200915194708htz&t=doc&p=esdu_71005d

35. ESDU 78020. Local buckling and crippling of I, Z and channel section struts. Engineering Sciences Data Unit; 1978. Available at: https://www.esdu.com/cgi-bin/ps.pl?sess=cranfield5_1200916222130srt&t=doc&p=esdu_78020

36. ESDU 84012. Buckling of thin-walled unstiffened circular cylinders under torsion and pressure. Engineering Sciences Data Unit; 1984. Available at: https://www.esdu.com/cgi-bin/ps.pl?sess=cranfield5_1200915052031nnq&t=doc&p=esdu_84012

37. ESDU 88034. Avoidance of buckling of some engineering elements (struts, plates and gussets). Engineering Sciences Data Unit; 1988. Available at: https://www.esdu.com/cgi-bin/ps.pl?sess=cranfield5_1200915052031nnq&t=doc&p=esdu_88034

38. Hughes AF., Iles DC., Malik AS. Design of Steel Beams in Torsion. SCI (The Steel Construction Institute). 2011.

39. Maddux GE., Giessler FJ., Vorst LA., Moritz T. Stress analysis manual. 1969. Available at: http://everyspec.com/USAF/USAF-General/AFFDL-TR-69-42_AUG1969_52363/

40. Raymer D. Aircraft Design: A Conceptual Approach, Sixth Edition. Aircraft Design: A Conceptual Approach, Sixth Edition. 2018. Available at: DOI:10.2514/4.104909

41. Hoerner SF. Fluid-dynamic Drag: Practical Information on Aerodynamic Drag and Hydrodynamic Resistance. Hoerner Fluid Dynamics (ed.) Midland Park, N.J.; 1965. 460 p.

42. Torenbeek E. Synthesis of subsonic airplane design : an introduction to the preliminary design, of subsonic general aviation and transport aircraft, with emphasis on layout, aerodynamic design, propulsion, and performance. Delft University Press; 1982. 598 p.

43. Roskam J. Airplane design. Ottawa, Kansas: Roskam Aviation and Engineering Corporation; 1990.

44. Vries HD. Development of a main landing gear attachment fitting using composite material and resin transfer moulding. 2009.

45. Rosa L. BAe 146 landing gear. 2007.

46. Airbus. ZEROe - Hydrogen - Airbus. 2020. Available at: https://www.airbus.com/innovation/zero-emission/hydrogen/zeroe.html (Accessed: 26 March 2021)

47. Thuis HGSJ (National AL. Composite landing gear components for aerospace applications. In: ICAS (ed.) 24th Congress of International Council of the Aeronautical Sciences. Yokohama, Japan: Optimage Ltd.; 2004. Available at: https://www.icas.org/ICAS_ARCHIVE/ICAS2004/ABSTRACTS/371.HTM

48. SAE A-5B Gears Struts and Couplings Committee. Development and Qualification of Composite Landing Gears. SAE International; 2020. Available at: DOI:https://doi.org/10.4271/AIR5552

49. Boyle A. How Boeing redesigned the landing gear to make the 737 MAX 10 fly. GeekWire. 2018. Available at: https://www.geekwire.com/2018/boeing-737-max-10-landing-gear/

50. Obrovsky FM. Design of a fuselage mounted main landing gear for a low wing A320 class aircraft. Individual Research Project MSc Thesis. Cranfield University; 2013.

51. Li X., Li Y. The Review and Development of the Landing Gear Emergency Release System. MATEC Web of Conferences. 2017; 114: 1–8. Available at: DOI:10.1051/matecconf/201711403016

52. SAE A-5B Gears Struts and Couplings Committee. Extraordinary and Special Purpose Landing Gear Systems. SAE International; 2012. Available at: DOI:10.4271/AIR4846A

53. Whitford R. Lessons Learned from the British Aircraft Corporation TSR2 Project. SAE International; 2000. Available at: DOI:https://doi.org/10.4271/2000-01-5514



https://dspace.org/

Impact of high-aspect-ratio wing aircraft concepts on conventional tricycle landing gear integration

Martin, Raphaël; Stockford, Jack; Smith, Howard

2025-05-10
Society of Automotive Engineers (SAE)
https://doi.org/10.4271/01-18-02-0008
Martin R, Stockford J, Smith H. (2025) Impact of high-aspect-ratio wing aircraft concepts on conventional tricycle landing gear integration. SAE International Journal of Aerospace, Volume 18, Issue 2, May 2025, SAE 01-18-02-0008

Downloaded from a DSpace repository. https://dspace.org/